Silicon Avalanche Photodiodes

A. Stoykov & R.Scheuermann,

Laboratory for Muon Spin Spectroscopy,

Paul Scherrer Institut, CH-5232 Villigen PSI, Switzerland

The first avalanche photodiodes (APD) were developed more than 40 years ago. For a long time APDs remained red and near-infrared sensitive detectors with an active area below 1 mm^2. During the last ten years a large progress has been made in the development of large area (tens of square millimeters) APDs sensitive to scintillation light in the blue and near-ultraviolet wavelength region. These APDs started to find their fields of application in experimental nuclear and particle physics. The most impressive example is the Electromagnetic Calorimeter of the CMS experiment at CERN, where more than 10^5 APDs (S8148 produced by Hamamatsu Photonics) will be used to detect scintillation light from PbWO$_4$ crystals [1].
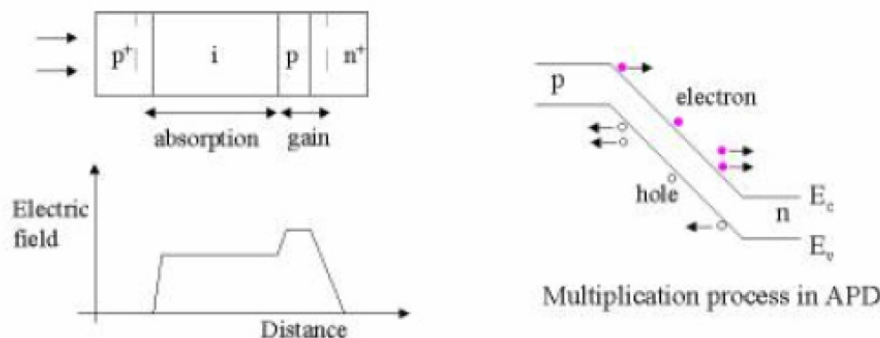

Figure 1. Illustration of the operation principle of an APD.

The operation principle of an APD is based on the conversion of the energy of photons (γ-quanta, ionizing particles) into free charge carriers in the semiconductor bulk and their further multiplication via the process of impact ionization. An example of the APD structure is shown on Figure 1. The basic element of the structure is the *p-n* – junction. Under the reverse bias an electric field exists in a certain volume of the device close to the junction, and this volume becomes depleted of free charge carriers. The charge carriers created in the depleted region drift in the electric field towards the corresponding electrodes. The feature distinguishing an APD from a photodiod (PD) is a build-in region with very high (>10^5 V/cm) electric field. The charge carriers traversing this region acquire enough energy to produce electron-hole pairs by impact ionization. The newly created charge carriers may create new ones, and so on. Thus there is an avalanche of electrons

and holes moving through the detector. These current pulses are then detected in an external circuit.

The APDs which are produced nowadays are very different in their design, internal structure, parameters, and accordingly find their application in different fields. The well known producers of APDs are:

Hamamatsu Photonics,

Advanced Photonics, Inc. (API),

Radiation Monitoring Devices, Inc. (RMD),

Perkin Elmer Optoelectronics (formerly EG&G).

Very promising APDs operating in Geiger mode are produced in Russia by the groups of Z.Sadygov (Dubna) and V.Golovin (Moscow). Examples of some APD types are shown in Figure 2.
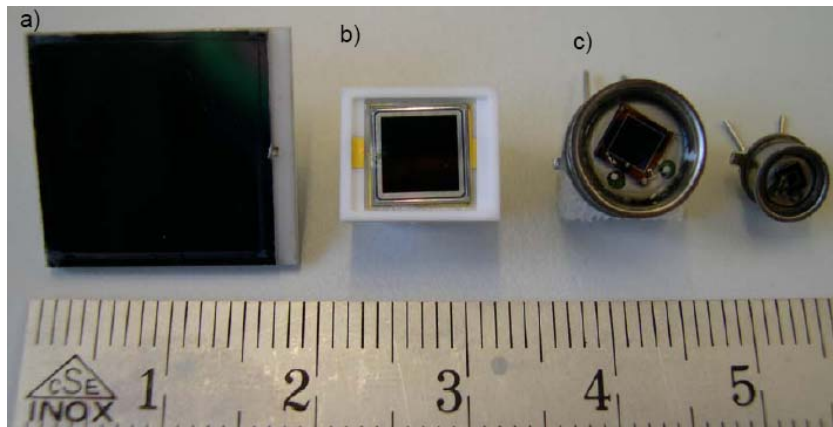

Figure 2. Examples of some state-of-the-art APDs:
a) RMD S1315 (13 x 13 mm^2); b) Hamamatsu S8148 (5 x 5 mm^2);
c) Dubna R8 AMPDs (2.75 x 2.75 mm^2 and 0.75 x 0.75 mm^2).

The basic parameters characterizing the operation of APDs are:
- quantum efficiency QE;
- avalanche gain M;
- excess noise factor F;
- dark current $I_d = I_s + M \cdot I_b$, where I_s and I_b are the surface leakage current and the bulk generation current respectively;
- capacitance C_d and series resistance R_s , which determine the response function of the APD;
- operating voltage U.

Figure 3 gives an example of the behavior of APD parameters. As is seen from the figure, the quantum efficiency of the APD is significantly higher than that of a PMT at $\lambda > 400$ nm (XP2020: QE ~20%).

The gain M increases as the reverse bias voltage U applied to APD approaches the breakdown voltage U_b:

$$M = 1 / (1 - (U / U_b)^n).$$

In vicinity of U_b a large current flows through the APD which might cause its permanent damage. By cooling of the APD it is possible to achieve higher gains due to the decrease of the bulk current.
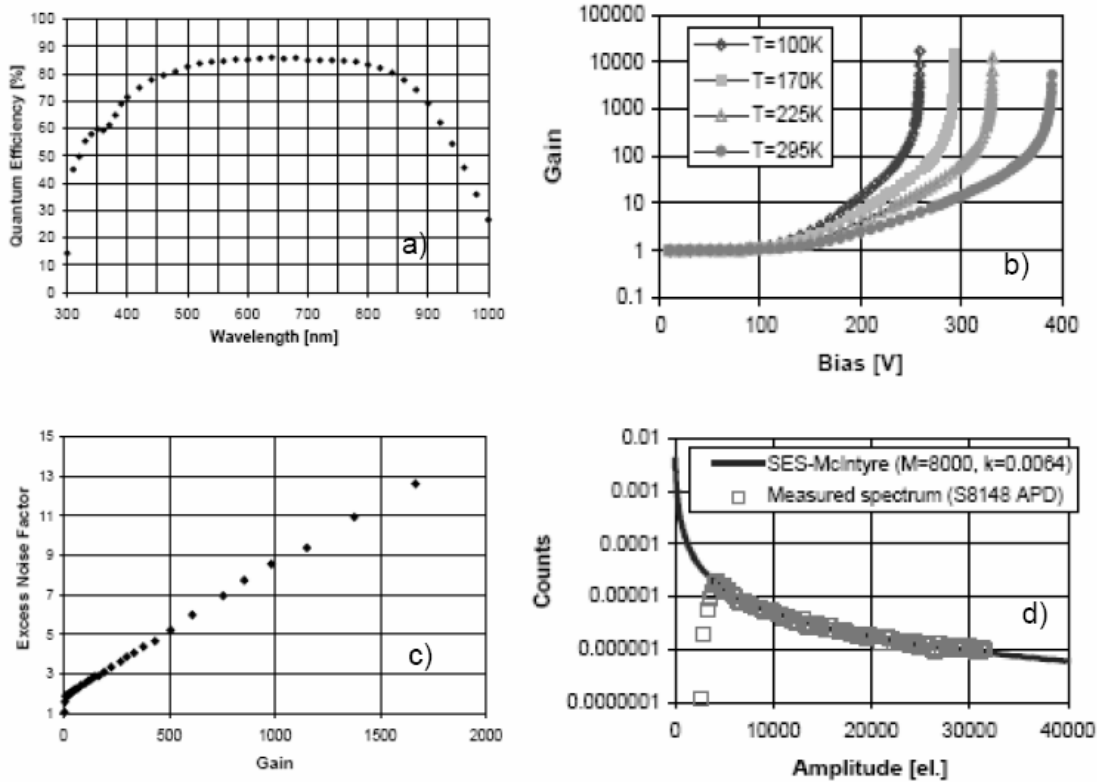

Figure 3. Some parameters [2,3] of the S8148 Hamamatsu APD:

a) quantum efficiency $QE(\lambda)$,

b) avalanche gain $M(U)$,

c) excess noise factor $F(M)$;

d) APD single electron spectrum: measured ($T = 108$ K, $M = 8000$) and calculated according to theory [4].

Since the avalanche multiplication is a random process, the APD is not an ideal amplifier – the number of charge carriers created per avalanche has a wide distribution (see Fig. 3d). To take this into account a so-called excess noise factor F is introduced:

$$F = \langle M^2 \rangle / \langle M \rangle^2$$

(for an ideal amplifier: $F = 1$). With increasing gain the excess noise factor increases as $F \approx 2 + kM$, where $k = \beta/\alpha$, α and β being the ionization coefficient for electrons and holes, respectively. Multiplication noise deteriorates the energy (amplitude) resolution of the APD:

$$\sigma^2(A) / A^2 \sim F / (N_{ph}\, QE),$$

where A, $\sigma(A)$, and N_{ph} are the amplitude of the detector signal, its variation, and the number of incident photons, respectively.

The S8148 considered above is an example of the so-called linear-mode APD, i.e., an APD operating in the proportional region of avalanche multiplication ($U < U_b$). Typical operating voltages of the linear-mode APDs are strongly dependent on their structure and are varied from about 100 to 1800 Volts (for beveled edge APDs).

A substantial increase of APD gain and thus its sensitivity becomes possible in multi-pixel APDs operating in the regime of Geiger breakdown. An example is the Avalanche Microchannel Photo Diode (AMPD) developed by the Dubna APD-group [5]. The AMPD is a matrix of microcells (micro-APDs) with dimensions from 5 to 30 μm. Each microcell operates above the breakdown voltage. The discharge currents from the cells are added on the common load resistor and the output signal of the device is the sum of the signals from all the cells firing at the same time. High density of the cells ($\sim 10^4$ mm^{-2}) makes the response of the device linear over a wide range of the light intensities.

Dubna R8 APD

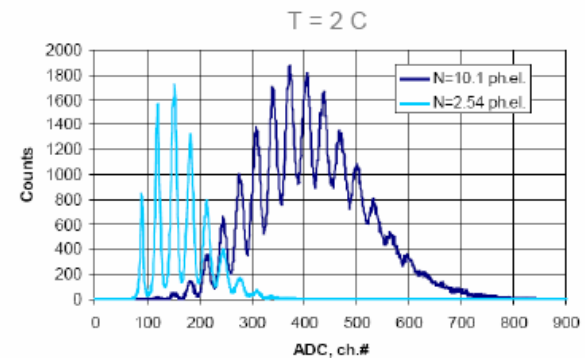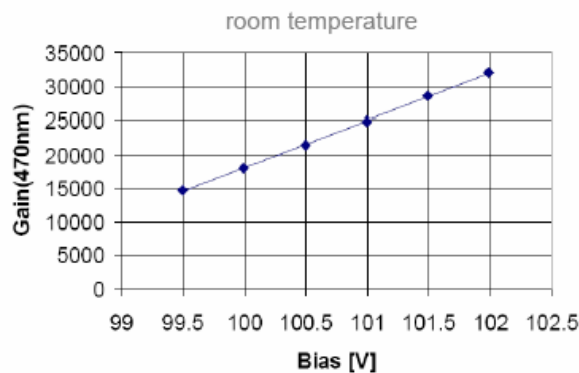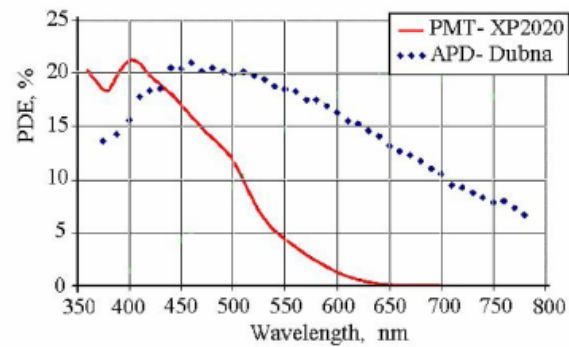|	
Active area:	0.75 x 0.75 mm^2
Operating voltage:	96 - 100 V
Gain:	20 000 - 30 000.
Dark Current:	20 - 30 nA (M=20 000)
Capacitance:	9 pF
Excess noise factor:	1 - 1.1

Figure 4. Characteristics of the R8 Dubna AMPD [6].

Figure 4 shows the characteristics of the Dubna R8 AMPD. The maximum gain of the device is about $3 \cdot 10^4$ and increases linearily with increasing over-voltage (U - U_b).

The amplitude distribution of the AMPD signals in response to illumination by weak light pulses (only few photons per pulse) consists of well defined peaks from one, two, etc. photoelectrons. The AMPD is practically an ideal amplifier: each photoelectron produces an output pulse of the same amplitude, and the excess noise factor of this device is close to 1. The consequence of the cell-like structure of the AMPD is that not all the charge carriers created by light in the bulk of the device enter the region of high electric field and trigger an avalanche. This reduces the photon detection efficiency (*PDE*) of the device compared to its quantum efficiency:

$$PDE = k_{geom} \cdot QE,$$

where k_{geom} is the geometry factor. As is seen from the figure the *PDE* of an R8 AMPD exceeds that of an XP2020 photomultiplier at $\lambda > 430 – 450$ nm.

Our interest to APDs aims at:

1. development of a position-sensitive coordinate detector (Beam Profile Monitor -- BPM);
2. development of the detector system for a High Magnetic Field (10 Tesla) μSR-spectrometer.
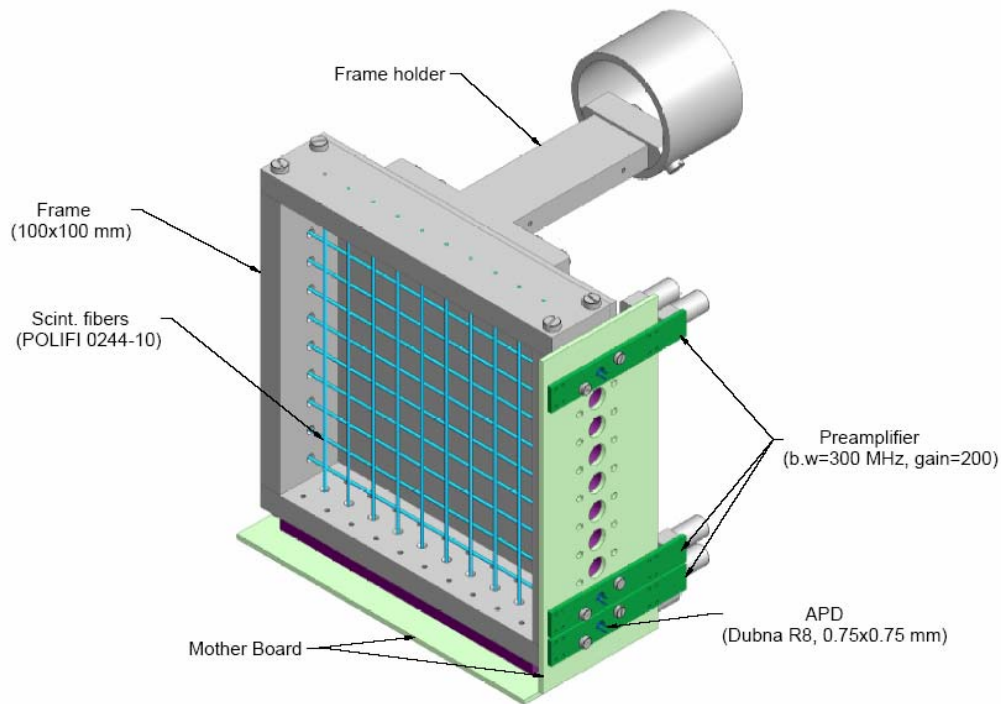

Figure 5. Beam Profile Monitor.

1) The BPM is essential for the optimization of the Avoided Level Crossing (ALC) spectrometer performance and will be used to determine the field dependence of the muon beam spot in order to find out the origin for the field-dependent variation of the asymmetry in this spectrometer. The BPM (see Figure 5) consists of a grid of 20 scintillating fibers (POLIFI 0244-10, λ = 430 nm, diameter 1 mm), 10 of which are mounted along the X-, and 10 along the Y-axis. The length of the fibers and the spacing are respectively 100 mm and 10 mm. A muon stopped in the fiber produces scintillation light (the estimated number of photons is ~ 300 per muon) which is registered by an AMPD (R8, Dubna) at the end of the fiber. The choice of the AMPD as photosensor for the BPM is conditioned by its high *PDE* at 430 nm and its high gain. Each AMPD is mounted on-board of an amplifier (gain ~200, bandwidth ~300 MHz). The use of a high gain APD with a fast amplifier is an essential requirement since the muon rate per channel might be as high as 10^6 s^{-1}. The electric scheme combining the AMPD biasing and the amplifier circuits is shown in Figure 6.
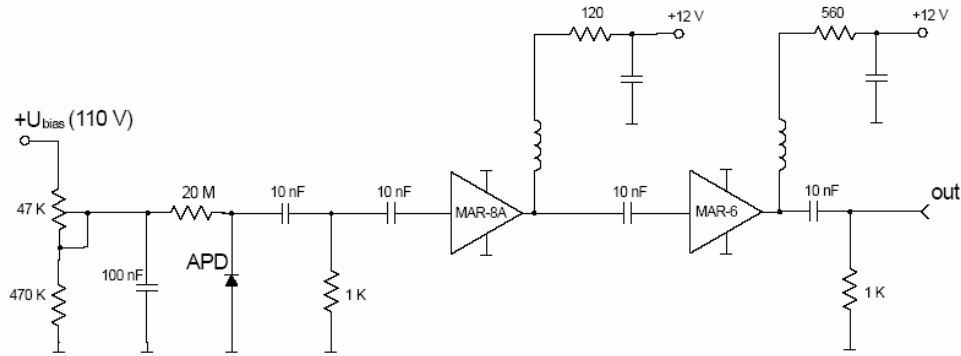

Figure 6. AMPD biasing and preamplifier circuits [7].

The scintillating fibers and AMPD-amplifier channels are mounted on an aluminum frame of dimension 120 x 120 mm^2. The BPM can be placed inside the ALC solenoid at the sample position and probe the beam intensities I_i and I_j at coordinates x_i and y_j of the fibers (i, j = 1...10). The X- and Y-distributions of the beam are calculated as:

$$W_i = I_i / \Sigma I_i, \; W_j = I_j / \Sigma I_j.$$

The total beam intensity can be estimated as $I_\mu \approx 10 \cdot \Sigma I_i \approx 10 \cdot \Sigma I_j$.

2) The main requirement for the detector to be used in the HMF μSR-spectrometer is the time resolution in the order of $\sigma = 50$ ps for detection of incident muons (the muon counter) and the decay positrons (the positron counter). Our interest in APDs in this context is conditioned by their immunity to high magnetic fields which makes it possible to

place the photodetector close to the scintillator and exclude the need of light guides (the time spread for the light passing through the light guide deteriorates the time resolution of the counter). Some APD types can also be used to detect muons and the decay positrons directly.

Following APDs we consider as promising candidates for the HMF μSR-spectrometer:

- Hamamatsu S8148: active area 25 mm^2, high *QE*. At room temperature *M* is not sufficiently high. The interest in this device lays in its operation at very low (LN2) temperatures, where a gain of one order of magnitude higher than at room temperature can be achieved.

- EG&G C30626F: active area 5 x 5 mm^2, Si wafer and the active thickness are about 140 μm. Can be used for direct detection of muons and positrons.

- RMD 8 x 8 mm^2 (S0814) and 13 x 13 mm^2 (S1315): sensitive-area devices with active thickness ~50 μm (but the Si wafer is ~300 μm thick). These devices might be useful for the direct detection of positrons. They are produced in a totally non-magnetic package.

- Dubna AMPD would be a good photosensor for the HMFμSR spectrometer provided that the following specification can be achieved: active area 25 mm^2, *PDE* > 20 % at 380 nm, *M* > 10^5.

Another device which might be a promising candidate to be used as a detector in the HMFμSR spectrometer is a Hybrid Avalanche Photodiode (HAPD), see Figure 7. The HAPD is a new detector that combines an electron tube and an APD. To detect low level light with a high S/N ratio, HAPD utilizes the "electron bombardment amplification method" by which photoelectrons emitted from the photocathode are accelerated by a high-intensity electric field to directly strike the avalanche photodiode (anode) where the electrons are multiplied.
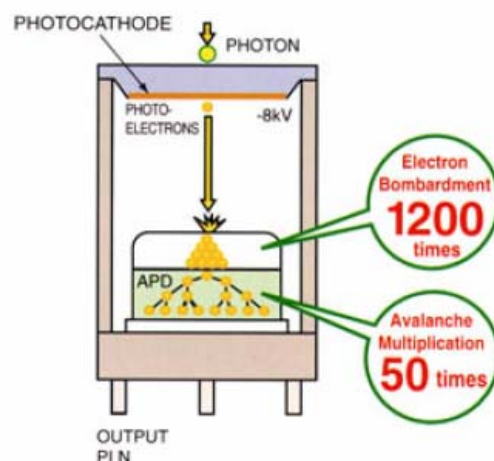

Figure 7. HAPD operation principle [8].

Advantages of an HAPD over a PMT are:

- very small (below 50 ps) transit time spread for the electrons passing from the cathode to the anode. The time resolution is limited by the amplifier noise and is inversely proportional to the signal amplitude [9]: $\sigma \sim 1/N_e$. As known (see also [9]) the time resolution of a PMT is limited by the transit time spread and is inversely proportional to the square root of the signal amplitude;
- if oriented with its axis parallel to the magnetic field, an HAPD is much less sensitive to the magnetic field than a PMT.

Our plans for this series of tests are:

1. study the operation of the BPM and use it to measure the field dependence of the muon-beam distribution in the ALC solenoid up to 5 Tesla;
2. study the performance of the Hamamatsu HAPD R7110U-07 in a magnetic field up to 5 Tesla;
3. study the operation of the RMD APDs at direct registration of positrons in the magnetic field up to 5 Tesla.

References

[1] Yu.Musienko, NIM A 494, 308 (2002).

[2] D.Renker, NIM A 486, 164 (2002).

[3] A.Dorokhov *et.al.*, NIM A 504, 58 (2003).

[4] R.J.McIntyre, IEEE Trans. Electron Devices, ED-19, 703 (1972).

[5] Z.Sadygov et.al., NIM A 504, 301 (2003);

    `http://sunhe.jinr.ru/struct/neeo/apd/index.html`.

[6] Data courtesy of Yu. Musienko (CERN).

[7] Ch. Buehler, U. Greuter, N. Schlumpf, PSI Report TM-14-02-01.

[8] `http://www.hpk.co.jp/eng/products/ETD/hpde/hpde.htm`.

[9] S.Matsui *et.al.*, NIM A 463, 220 (2001).